

Supporting Information

Ambipolar organic field-effect transistors with balanced mobilities through solvent-vapour annealing induced phase-separation of bi-component mixtures

Matthias Treier,^a Jean-Baptiste Arlin,^b Christian Ruzié,^b Yves H. Geerts,^b Vincent Lemaur,^c Jérôme Cornil,^c and Paolo Samori^{*a}

^a Nanochemistry Laboratory, ISIS, CNRS 7006, Université de Strasbourg, 8 allée Gaspard Monge, 67000, Strasbourg, France; E-mail: samori@unistra.fr

^b Laboratoire de Chimie des Polymères, CP 206/01, Faculté des Sciences Université Libre de Bruxelles (ULB), Boulevard du Triomphe, 1050 Brussels, Belgium

^c Service de Chimie des Matériaux Nouveaux, Université de Mons (UMons), Place du Parc 20, 7000 Mons, Belgium

X-ray diffraction study

Specular X-ray Diffraction (sXRD) was performed on a Bruker D8 diffractometer using Cu K α radiation ($\lambda=1.5418 \text{ \AA}$). Diffraction patterns were collected at room temperature in the scattered range 1.6-40° with angular resolution 0.02° per step, counting time per step were of 5s for powder samples (Figures S1 and S2) and 10s for spin-coated materials on silicon wafers (Figures S4 and S5), using a 0/0 reflection geometry. All sXRD patterns are represented in counts versus 2θ values.

Powder materials

Compound 2B

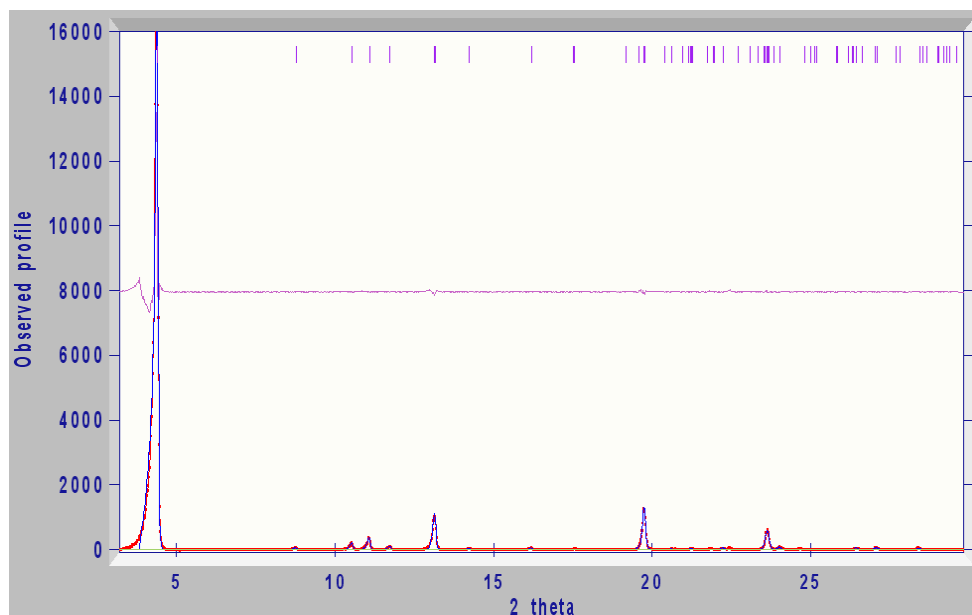


Figure S1: XRPD data shown in the range 3 – 29.9° 2θ, Pawley [1] fitted ($\chi^2 = 6.326$) to published unit cell from PDI 2B. Refined unit cell parameters using DASH [2] program in triclinic space group P-1 are: a , b , $c = 4.690$, 8.543 , 20.302 \AA and α , β , $\gamma = 85.124$, 88.057 , 80.939° .

The red line is the measured profile, the blue line is the calculated profile and the purple line is the difference between the two. The refined unit cell parameters are in good agreement with the published low temperature unit cell [3]. The (001) reflection is the most intense reflection for a 2θ value of 4.388° .

Compound 1A

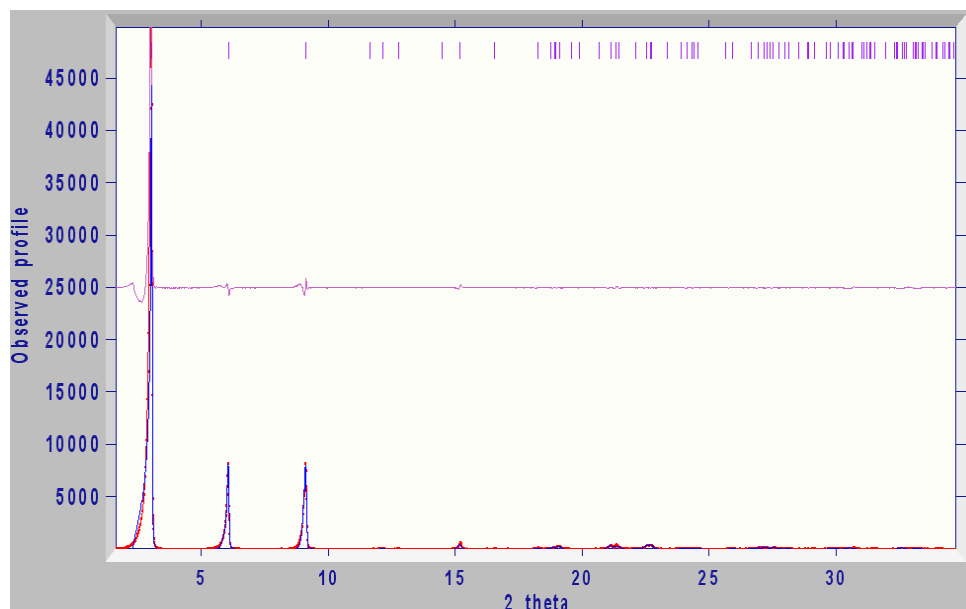


Figure S2: XRPD data shown in the range $1.6 - 34.9^\circ 2\theta$, Pawley fitted ($\chi^2 = 26.648$) to published unit cell⁴. Refined unit cell parameters using DASH program in monoclinic space group P2₁/a: $a, b, c = 5.911, 7.894, 29.216 \text{ \AA}$ and $\beta = 91.98$.

The refined unit cell parameters are in good agreement with the published unit cell. The (0 0 1) reflection is the most intense reflection for a 2θ value of 3.059° . This reflection being under fitted gave a rather high Pawley χ^2 .

For both Pawley fitted powder patterns of both **1A** and **2B**, no additional peaks other than the ones corresponding to the expected unit cell can be observed, thus showing the crystalline phase purity of the material used.

Spin-coated thin films on SiO₂

The results are only shown in the scattered range 2 to 20° as there was no diffraction peaks observed for higher 2θ values. For low values of θ , the background is quite high in figures S4 and S5 due to x-ray scattered from the silicon wafer (see figure S3), but no diffraction peak can be observed.

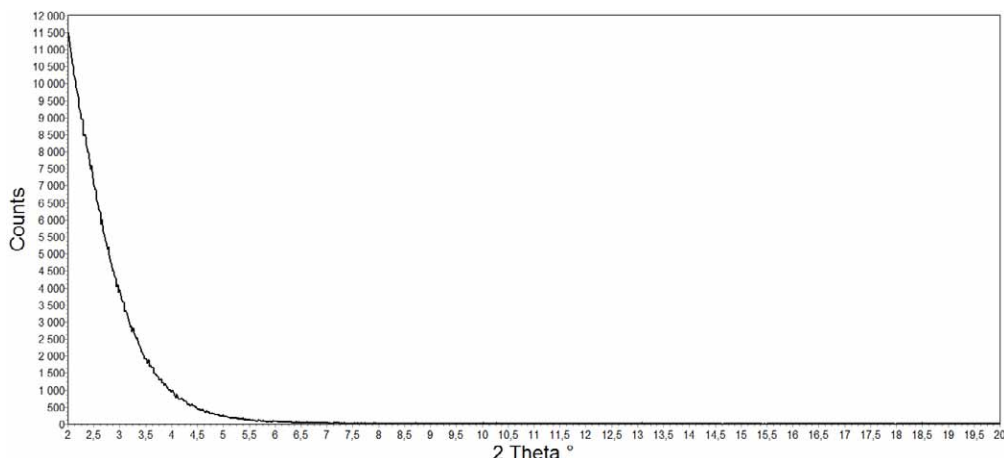


Figure S3: sXRD data shown in the range 2-20° 2θ from an untreated silicon wafer.

For thin films obtained by spin-coating **1A**, **2B** or a mixture of both on a silicon wafer broad diffraction peaks are observed. Figure S4 shows an overlay of sXRD patterns obtained for thin films **2B** (red), **1A** (blue) and the mixture (purple) before SVA treatment. For **2B**, only a very broad hump can be observed at 3.06°. For **1A**, three broad diffraction peaks can be observed at 2.95°, 6.03°, 9.17° with an average full width at half maximum (FWHM) of 0.32°.

For the mixture of both compounds, the hump observed for **2B** sample is convoluted with the first diffraction peak seen for **1A** thus giving a broader peak than the one observed for **1A** alone (FWHM of 0.35° at 3.00°) the two other diffraction peak are still observed at 6.06° and 9.16 ° (average FWHM of 0.25°).

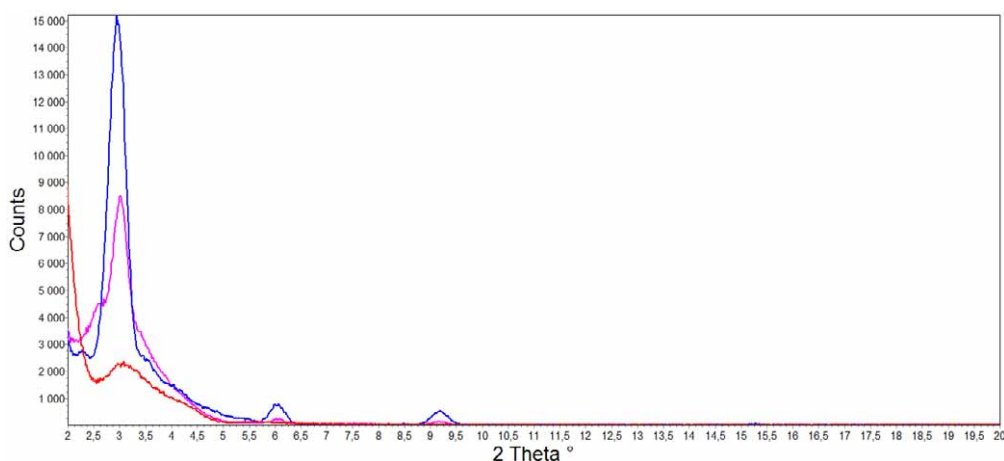


Figure S4: sXRD data shown in the range 2-20° 2θ from spin-coated films of **2B** (red), **1A** (blue) and the mixture (purple) on a silicon wafer without SVA treatment.

After SVA sharper and more intense diffraction peaks are observed (see figure S5). For **2B**, a broad diffraction peak at 4.26° is observed with a FWHM of 0.39°. For **1A**, three sharp diffraction peaks can be observed at 3.07°, 6.11° and 9.15 ° with an average FWHM 0.06°. For the mixture, three sharp diffraction peaks with the same d-spacing as the one for **1A** alone can be observed and a broad diffraction peak at 4.38° (due to **2B**) with a FWHM of 0.37°.

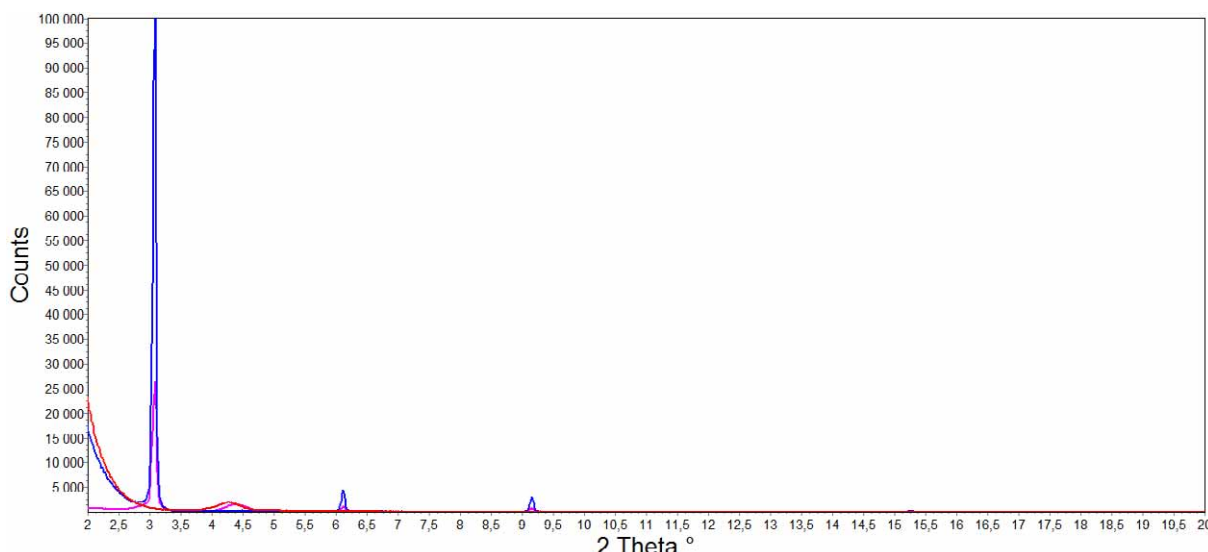


Figure S5: XRPD data shown in the range $2\text{--}20^\circ 2\theta$ from spin-coated thin films after SVA in THF: **2B** (red), **1A** (blue) and the mixture (purple).

Conclusion on the X-ray study

The SVA treated samples all show a great improvement in the crystallinity compared to the as-spin-coated films, this is seen from the gain of intensity and the greater sharpness of the diffraction peaks. The phase separation of PDI **2B** and BTBT **1A** is also underlined by the fact that the SVA treated spin-coated mixture pattern, matches with the addition of both patterns from SVA samples of each compound alone. The only little misfit in the addition is a small peak shift for the PDI between the PDI alone or within the mixture. This misfit could be explained by the fact the PDI crystallites have grown larger in the mixture sample. From the specular XRD measurements, it can also be determined that both compounds have their $\{001\}$ faces lying parallel to the substrate and thus have their alkyl chains coming out of it and their long molecular axes along the substrate normal. These $\{001\}$ plane d spacing values are the same as the one from the unit cell of the raw materials, and thus their known crystal structures. This orientation also allows for efficient charge carrier pathways parallel to the substrate surface which is in good agreement with the OFET results.

Morphology study

The crystal growth for **1A** and **2B** has been characterized from the crystal structures, determined by *Briseno et al* [3] and *Isawa et al* [4] respectively, using the Morphology module of the Materials Studio package [5] (using the COMPASS force field [6]). The attachment energy (E_{att}) method developed by Hartmann [7] has been used to determine the relative importance of the different crystallographic faces in the crystal morphology: faces with higher E_{att} in absolute value grow faster and have then less importance in the final crystal shape (see tables S1 and S2).

Table S1: Attachment energies and corresponding percentage in total facet area of the most dominant faces in the crystal shape of PDI **2B**

<i>hkl</i>	d _{hkl} (Å)	E _{att} (kJ/mol)	% total facet area
{ 0 0 1}	19.66	-33.22	73.59
{ 0 1 0}	8.42	-161.08	5.09
{ 1 0 0}	4.64	-282.00	1.89
{ 1 1 0}	4.29	-240.71	6.89
{ 0 1 2}	6.62	-137.40	3.81
{ 0 1 1}	7.93	-156.73	0.43
{ 0 2 1}	4.17	-161.13	0.02
{ 1 0 -2}	4.16	-263.09	0.59

Table S2: Attachment energies and corresponding percentage in total facet area of the most dominant faces in the crystal shape of BTBT **1A**

<i>hkl</i>	d _{hkl} (Å)	E _{att} (kJ/mol)	% total facet area
{ 0 0 1}	29.15	-25.60	81.11
{ 0 1 1}	7.61	-179.12	8.95
{ 1 1 1}	4.65	-265.48	9.95

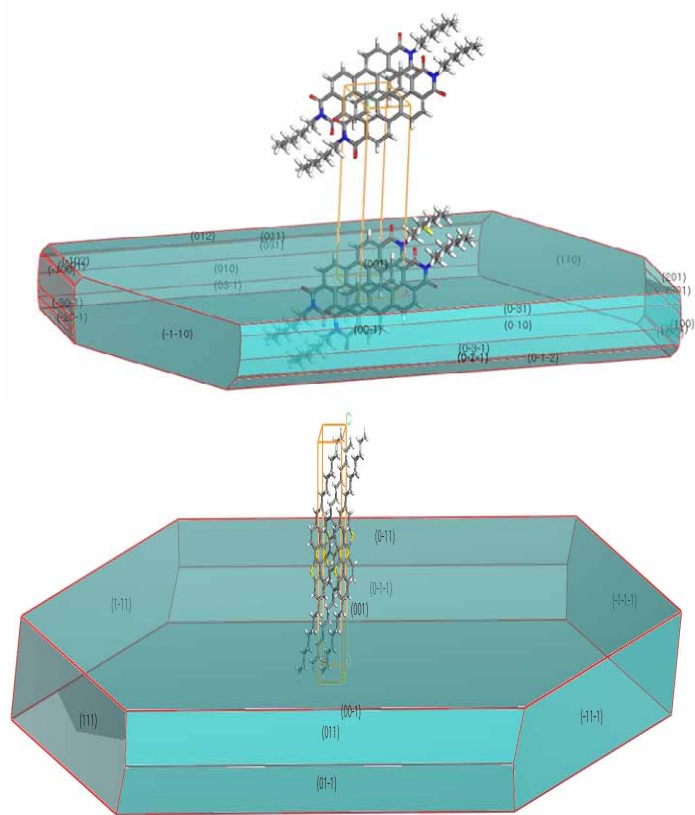


Figure S7: Pictures of calculated morphology for PDI-2B(left) and BTBT-1C(right)

From the calculations, both compounds are expected to have a plate like crystal morphology. It was clearly observed for the **1A** crystal on AFM images, however the **2B** crystals exhibited a needle-like morphology, implying that the morphology grown using SVA treatment did not produce in this case the kinetically expected morphology.

Output characteristics before and after SVA

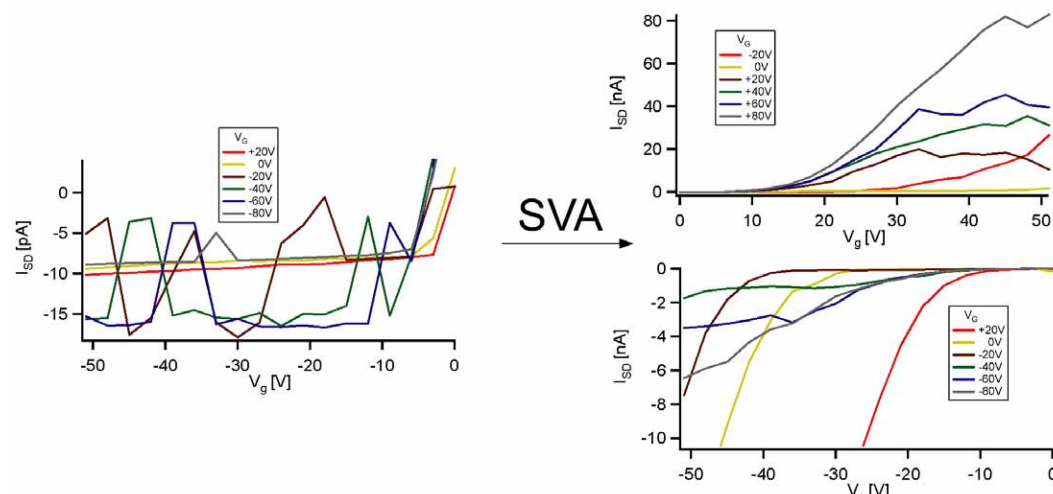


Figure S8: Output characteristics of a mixed BTBT/PDI OFET before (left) and after (right) SVA in THF. Before SVA the measured current is at the detection limit (hence the fluctuations) while the ambipolar characteristics are clearly observed after SVA

References

1. G. Pawley, in *Journal of Applied Crystallography*, Editon edn., 1981, vol. 14, pp. 357-361.
2. W. I. F. David, K. Shankland, J. van de Streek, E. Pidcock, W. D. S. Motherwell and J. C. Cole, in *Journal of Applied Crystallography*, Editon edn., 2006, vol. 39, pp. 910-915.
3. A. L. Briseno, S. C. B. Mannsfeld, C. Reese, J. M. Hancock, Y. Xiong, S. A. Jenekhe, Z. Bao and Y. Xia, *Nano Letters*, 2007, **7**, 2847-2853.
4. T. Izawa, E. Miyazaki and K. Takimiya, *Advanced Materials*, 2008, **20**, 3388-3392.
5. Materials Studio v5.0.0.0, Accelrys Software Inc., San Diego, 2009.
6. H.J. Sun, Phys. Chem. B 1998, **102**, 7338-7364
7. P. Hartman and P. Bennema, *Journal of Crystal Growth*, 1980, **49**, 145-156.